Journal of Ceramic Processing Research. Vol. 17, No. 12, pp. 1215~1218 (2016)

J O U R N A L O F
Ceramic
Processing Research

Pulsed current activated synthesis and consolidation of nanostructured Al-SiC composite and its mechanical properties

In-Jin Shon[a,*] and Woo-Jeong Kim[b]

[a]*Division of Advanced Materials Engineering, the Research Center of Advanced Materials Development, Chonbuk National University, 664-14 Deokjin-dong 1-ga, Deokjin-gu, Jeonju, Jeonbuk 561-756, Korea*

[b]*WONJIN ALUMINIUM, Technovalley-ro 416, Bongdong-eup, Wanju-gun, Jeollabuk-do, Korea*

Nanopowders of Si and Al_4C_3 were fabricated using high energy ball milling. The average grain sizes of Al_4C_3 and Si measured using X-ray diffraction patterns were lower than 50 nm, respectively. Highly dense nanostructured Al-SiC composite was simultaneously synthesized and consolidated within short time from the mechanically activated powders using pulsed current activated heating. The microstructure and mechanical properties (hardness and fracture toughness) of the Al-SiC composite were evaluated.

Key words: Sintering, Composite, Nanomaterial, Mechanical properties, Synthesis.

Introduction

Al alloys show an attractive properties of high conductivity, high toughness and low density for automotive and aerospace industries. Moreover, the strength of Al alloy was improved by reinforcing Al with the metal carbides. However, the ceramic reinforced Al composites exhibit high strength with low elongation which limited wide engineering applications [1-3]. The mechanical properties (strength and elongation) can be improved simultaneously by fabrication of nanostructured composite [4-7]. Recently, nanocrystalline powders have been developed by thermochemical and thermomechanical processes such as the spray conversion process (SCP), co-precipitation, high energy milling and electrical wire explosion [8-10]. Among the methods, high energy ball milling by repetitive cold-welding, fracture and dynamic recrystallization mechanism can provide driving force for activated inter-diffusion among the powders [11, 12]. However, the grain sizes of sintered materials are much larger than those of pre-sintered powders due to rapid grain growth that occurs during conventional sintering. Controlling grain growth during sintering is a key to the commercial success of nanostructured materials. Pulsed current activated sintering, which can produce densely nanostructured materials within short time, is effective for blocking grain growth [13-15].

The purpose of this work is to simultaneously synthesize and consolidate nanostructured 4Al-3SiC composite within five min from mechanically milled powders (Al_4C_3 and 3Si) by pulsed current activated sintering and to evaluate its mechanical properties and microstructure.

*Corresponding author:
Tel : +82-63-270-2381
Fax: +82-63-270-2386
E-mail: ijshon@chonbuk.ac.kr

Experimental Procedure

Powders of 99% pure Al_4C_3 (−325 mesh, Alfa, Inc) and 99.9985% pure Si (< 20 μm, Alfa, Inc) were used as a starting materials. Al_4C_3 and 3 Si powders were mixed by a high-energy ball mill, Pulverisette-5 planetary mill at 250 rpm and for 10 h. Tungsten carbide balls (9 mm in diameter) were used in a sealed cylindrical stainless steel vial under argon atmosphere. The weight ratio of ball-to-powder was 30:1.

After milling, the mixed powders were placed in a graphite die (outside diameter, 35 mm; inside diameter, 10 mm; height, 40 mm) and then introduced into the pulsed current activated sintering system made by Eltek in South Korea shown schematically in Ref. [16]. The four major stages in the sintering are as follows. The system was evacuated (stage 1) and a uniaxial pressure of 80 MPa was applied (stage 2). A pulsed current was then activated and maintained to 1450 °C with heating rate of 800 °C/min and then turned off without holding time (stage 3). The temperatures were measured using a pyrometer focused on the surface of the graphite die. At the end of the process, the sample was cooled to room temperature (stage 4). The process was carried out under a vacuum of 15 Pa.

The relative densities of the sintered sample were measured by the Archimedes method. Microstructural information was obtained from product samples which were polished. Compositional and microstructural analyses of the products were made through X-ray diffraction (XRD) and scanning electron microscopy (SEM) with

energy dispersive X-ray analysis (EDAX). Vickers hardness was measured by performing indentations at load of 20 kg and a dwell time of 15 s on the sintered samples. The grain size of the composite was calculated by Suryanarayana and Grant Norton's formula [17].

Results and Discussion

Fig. 1 shows FE-SEM images of raw materials of Al (a), Si (b), and FE-SEM image (c) and EDS analysis (d) of milled powders. All powders have irregular shape and milled powders are agglomerated. In EDS, the peaks of Si, C and Al were analyzed and there are no other peaks, such as Fe or W, which can possibly happen during the milling process. The X-ray diffraction pattern of mechanically high energy ball milled powders from raw powders is shown in Fig. 2. Products (Al and SiC) were not observed and reactants of Al_4C_3 and Si were detected. From this result, solid replacement reaction completely did not established during the high energy ball milling. The full width at half-maximum (FWHM) of the diffraction peak in Fig. 2 is broad due to refinement of powder and strain. The average grain

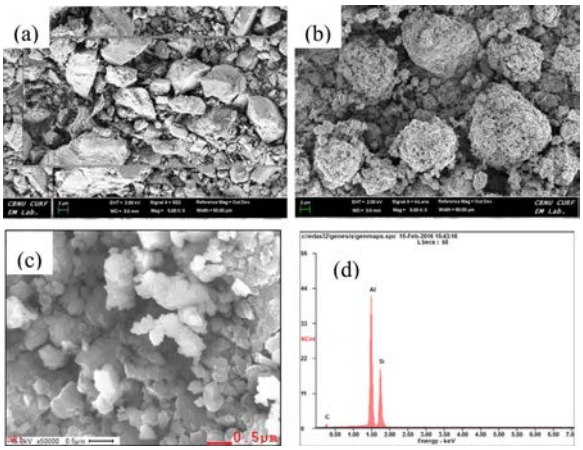

Fig. 1. FE-SEM images of raw material of Al (a), Si (b), and FE-SEM image (c) and EDS (d) of milled powders.

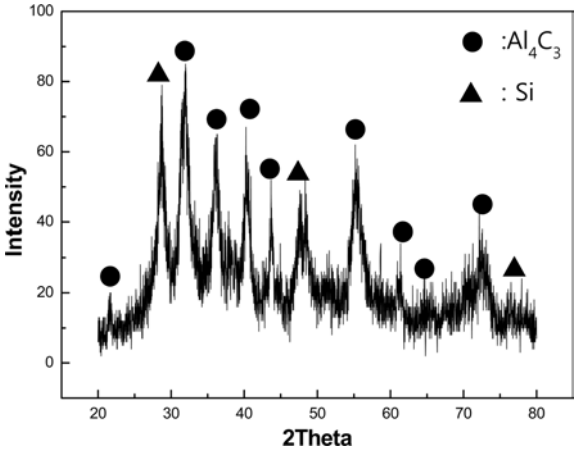

Fig. 2. XRD pattern of mechanically milled powders.

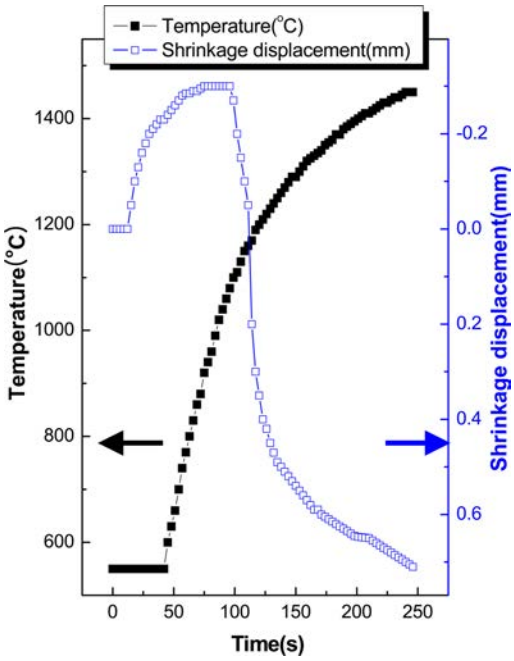

Fig. 3. The variation of temperature and shrinkage displacement with heating time during the synthesis and sintering of Al_4C_3+3 Si powders.

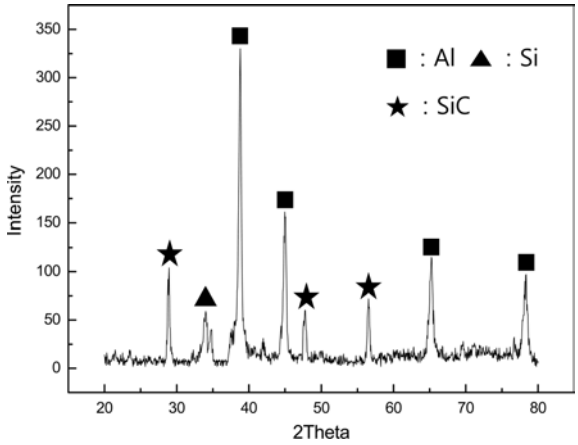

Fig. 4. XRD pattern of 4Al-3SiC composite sintered from high energy ball milled powders.

sizes of Al_4C_3 and Si measured by Suryanarayana and Grant Norton's formula were about 33 and 18nm, respectively. Fig. 3 shows the variation of temperature and shrinkage displacement with heating time during densification of milled powders. The application of the pulsed current resulted in shrinkage, due to synthesis and consolidation. As the pulsed current was applied, thermal expansion was shown up to 1050 ºC, and then shrinkage displacement rapidly increased above that temperature. XRD pattern of the high-energy ball milled powder heated to 1450 ºC is shown in Fig. 4. Al and SiC peaks are mainly detected. From the X-ray diffraction pattern, the interaction between Al_4C_3 and 3 Si, i.e.,

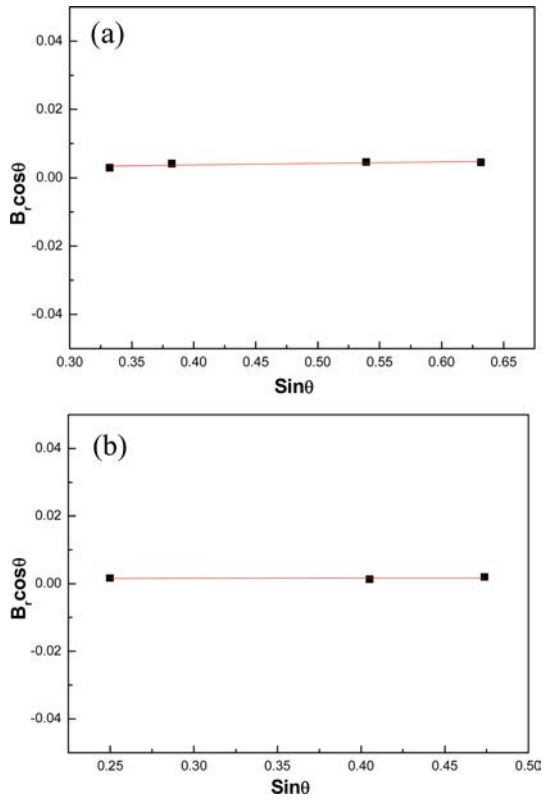

Fig. 5. Plot of $B_r\cos\theta$ versus $\sin\theta$ of (a) Al, and (b) SiC in sintered composite.

$$Al_4C_3 + 3\ Si \rightarrow 4\ Al + 3\ SiC \quad (1)$$

is thermodynamically feasible.

Fig. 5 shows plot of $B_r\cos\theta$ versus $\sin\theta$ to calculate grain size of Al and SiC in composite. The average grain sizes of Al and SiC in composite obtained from X-ray data in Fig. 4 by Suryanarayana and Grant Norton's formula, are 70, 98 nm, respectively. FE-SEM image and X-ray mapping of 4Al-3SiC composite sintered at 1450 ºC are shown in Fig. 6. The composites consist of nanograins. Dark area and grey area in FE-SEM are SiC and Al from EDS analysis and mass contrast, respectively. And the relative density of the 4Al-3SiC composite was 98%. It is considered that the reasons of high density of the composite obtained within five min are as follows. Firstly, the application of pressure during sintering increases driving force [18]. Secondly, the pulsed current enhanced sintering because of the fast heating due to Joule heating, the presence of plasma in pores separating powder particles, the enhancement of wettability and the rapid diffusion due to electromigration [19-21].

Vickers hardness measurements were made on polished sections of the 4Al-3SiC composite using a 20 kg_f load and a 15 s dwell time. The calculated hardness value of 4Al-3SiC composite sintered at 1450 ºC from high energy ball milled powders were 740 kg/mm^2. These values represent an average of five measurements.

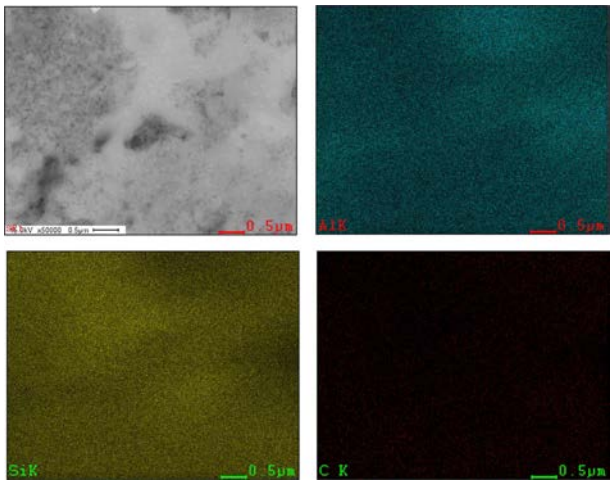

Fig. 6. FE-SEM image and X-ray mapping of 4Al-3SiC composite sintered from high energy ball milled powders.

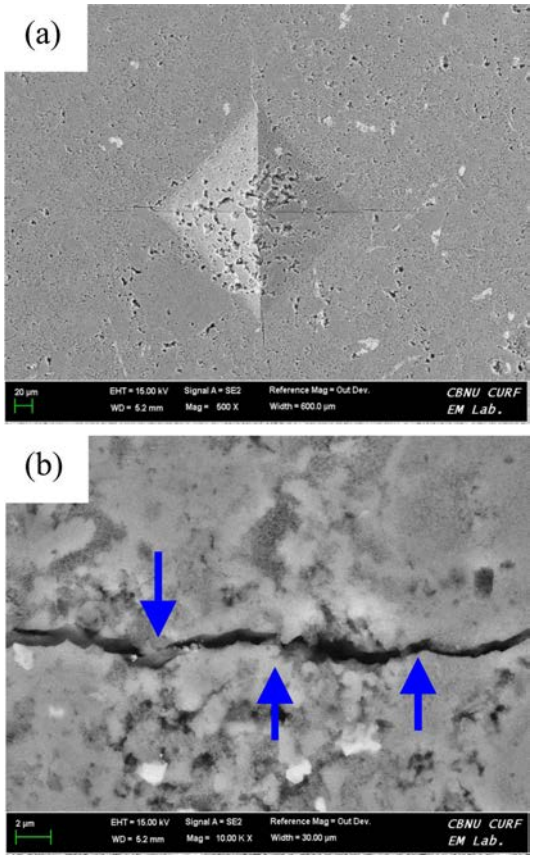

Fig. 7. (a) Vickers hardness indentation and (b) median crack propagating in the 4Al-3SiC composite.

Indentations with large enough loads produced median cracks around the indentation. The length of these cracks permits an estimation of the fracture toughness of the material. From the length of these cracks, fracture toughness values can be determined using by Anstis *et al.* **[**22**]** is

$$K_{IC} = 0.016\ (E/H)^{1/2} \cdot P/C^{3/2} \quad (4)$$

where E is Young's modulus, H the indentation hardness,

P the indentation load, and C the trace length of the crack measured from the center of the indentation. The modulus was estimated by the rule of mixtures for the 0.52 volume fraction of Al and the 0.48 volume fraction of SiC using E(Al)=71.9 GPa [23] and E(SiC)=439.9 Gpa [23]. As in the case of hardness values, the toughness values were derived from the average of five measurements. The toughness value of composite sintered from high energy ball milled is 9.5 $MPa \cdot m^{1/2}$.

A typical indentation pattern for the 4Al-3SiC composite is shown in Fig. 7(a). Typically, one to three additional cracks were observed to propagate from the indentation corner. A higher magnification view of the indentation median crack in the composite is shown in Fig. 7(b). This shows that the crack propagates in a deflective (↑) and branching (↓) manner. This is believed to suggest that Al and SiC in the composite may deter the propagation of cracks. The fracture toughness of 4Al-3SiC composite is greatly higher than that of monolithic SiC reported as 2 $MPa \cdot m^{1/2}$ [24].

Conclusions

Nanopowders of Al_4C_3 and Si were made using high energy ball milling for 10 h. The nanostructured 4Al 3SiC composite was simultaneously synthesized and consolidated from mechanically activated powders (Al_4C_3 and 3Si) within duration of five minutes using pulsed current activated heating. The average grain sizes of Al and SiC in composite obtained from X-ray data by Suryanarayana and Grant Norton's formula, are 70, 98 nm, respectively. The average hardness and fracture toughness values of the composite were 740 kg/mm^2 and 9.5 $MPa \cdot m^{1/2}$, respectively. The fracture toughness of the 4Al-3SiC composite is higher than that of monolithic SiC due to deterring crack propagation by Al and SiC.

Acknowledgments

Trade, Industry and Energy (MOTIE) and Korea Industrial Complex Corporation (KICOX) through the Industrial Complex (R & BD) Capacity Enhancement (Project Name: Development of high-strength (350 MPa) composite materials through waste recycling, Project Number: RHN16035) and this research was supported by Basic Science Research Program though the National Research Foundation of Korea (NRF) funded by the Ministry of Education (2015R1D 1A1A01056600) and this work was supported by the Korea Institute of Energy Technology Evaluation and Planning (KETEP) and the Ministry of Trade, Industry & Energy (MOTIE) of the Republic of Korea (No. 20164030201070).

References

1. Q.C. Jiang, X.L. Li, and H.Y. Wang, Scr. Mater. 48 (2003) 713-717.
2. X.C. Tong and A.K. Ghosh, J. Mater. Sci. 36 (2001) 4059-4069.
3. F. Tang, M. Hagiwara, and J.M. Schoenung, Mater. Sci. Eng. A 407 (2005) 306-314.
4. M. Bahrami, K. Dehghani, and M.K.B. Givi, Mater. Des. 53 (2014) 173-178.
5. D.S. Zhou, F. Qiu, H.Y. Wang, and Q.C. Jiang, Acta Metall. Sin. (Engl. Lett.) 27 (2014) 798-805.
6. G. Cao, H. Honishi, and X. Li, Mater. Sci. Eng. A 486 (2008) 357-362.
7. Bong-Won Kwak, Seung-Jin Oh, Byung-Su Kim, Jin-Kook Yoon, and In-Jin Shon, Korean J. Met. Mater. 54 (2016) 180-186.
8. Bong-Won Kwak, Seok-Jae Lee, and In-Jin Shon, Korean J. Met. Mater. 54 (2016) 409-414.
9. In-Jin Shon, Hyoung-Gon Jo, Byung-Su Kim, Jin-Kook Yoon, and Kyung-Tae Hong, Korean J. Met. Mater. 53 (2015) 474-479.
10. A.I.Y. Tok, L.H. Luo, and F.Y.C. Boey, Mater Sci. Eng. A. 383 (2004-2005) 229-234.
11. Suryanarayana, C., Progress in Materials Science 46 (2001) 1-184.
12. Kursun, C. and Gogebakan, M. Journal of Alloys and Compounds 619 (2015) 138-144.
13. So-Mang Kwon, Na-Ra Park, Jae-Won Shin, Se-Hoon Oh, Byung-Su Kim, and In-Jin Shon, Korean J. Met. Mater. 53 (2015) 555-562.
14. Bo-Ram Kang, Jin-Kook Yoon, Kyung-Tae Hong, and In-Jin Shon, Met. Mater. Int. 21[4] (2015) 698-703.
15. Bo-Ram Kang and In-Jin Shon, Korean J. Met. Mater. 53 (2015) 320-325.
16. Bong-Won Kwak, Byung-Su Kim, Jin-Kook Yoon, Kyung-Tae Hong, and In-Jin Shon, Journal of Ceramic Processing Research 16[3] (2015) 340-345.
17. C. Suryanarayana and M. Grant, Norton, X-ray Diffraction A Practical Approach, Plenum Press, New York, 1998.
18. R.L. Coble, J. Appl. Phys. 41 (1970) 4798-4807.
19. Z. Shen, M. Johnsson, Z. Zhao, and M. Nygren, J. Am. Ceram. Soc. 85 (2002) 1921-1927.
20. Yan Gu, Ping Shen, Nan-Nan Yang, and Kang-Zhan Cao, Journal of Alloys and Compounds 586 (2014) 80-86.
21. J.E. Garay, U. Anselmi-Tamburini, Z.A. Munir, S.C. Glade, and P. Asoka-Kumar, Appl. Phys. Lett. 85 (2004) 573-575.
22. G.R. Anstis, P. Chantikul, B.R. Lawn, and D.B. Marshall, J. Am. Ceram. Soc. 64 (1981) 533-538.
23. Shackelford, James F. Materials Science and Engineering Hand book Ed. James F. Shackelford & W. Alexander Boca Raton: CRC Press LLC, 2001.
24. In-Jin Shon, Hyun-Su Kang, Na-Ra Park, and In-Yong Ko, Advanced Materials Research Vols. 123-125 (2010) 635-638.